E-4

EFFECT OF HYDROGEN ENVIRONMENT ON CREEP AND FRACTURE OF STEELS

F. H. Vitovec[1]

Abstract

The effects of hydrogen environment at increased pressure on the mechanical properties of steels were investigated at temperatures above those at which low-strain rate embrittlement is observed.

Carbon steels, low alloy steels and stainless steels were subjected in unstressed condition for different periods to purified hydrogen at pressures of 28 atm., 63 atm., and 100 atm. and at temperatures of 425°C, 540°C and 594°C. Creep tests were conducted under identical environmental conditions. The behavior of the steels in hydrogen environment was compared with that in argon at 3 atm. pressure at the same test temperatures.

The behavior of the carbon steel and the low alloy steels is characterized by the chemical reaction of hydrogen and carbon to form methane at preferred sites along grain boundaries resulting in gas bubbles and fissures. An applied stress influences the kinetics of this attack. For carbon and low alloy steels hydrogen attack and decarburization are accelerated by creep stress. The rupture time is significantly reduced and the creep rate increased by high pressure hydrogen environment. A steel which has been decarburized prior to exposure and a 12% chromium steel were not affected by the environmental conditions used in this investigation. The rupture times of an austenitic stainless steel were slightly increased by hydrogen.

Introduction

The effects of a gaseous environment on the creep properties of metals may result from an interaction of the gas with the mechanisms of creep deformation or those of nucleation and propagation of cracks. The interaction may be limited to the surface and may be caused by a change of the surface energy or by a chemical reaction of the gas

---

(1) University of Alberta, Edmonton, Alta., Canada. This work was performed while the author was associated with the University of Wisconsin, Madison, Wis., U. S. A.

with a constituent of the alloy. Such interactions may also occur within the material. In this case the gas must be absorbed into the metal. It may act as a solute or it may react with a constituent of the alloy to form a solid or gaseous precipitate.

When carbon steel is exposed to a hydrogen environment at elevated temperature methane is formed by a reaction of hydrogen with the carbon of the steel. The reaction may occur entirely at the specimen surface to produce decarburization only or at internal interfaces such as grain boundaries, thereby creating fissures which induce embrittlement of the macroscopic section and cause a loss of strength, swelling, and decarburization. At low partial hydrogen pressures the reaction occurs mainly at the surface. Increasing the hydrogen pressure increases the extent of the internal reaction which causes hydrogen attack.

The kinetics of attack and the formation and growth of the fissures are usually indicated indirectly by the changes of the physical properties as a function of time of exposure to hydrogen (1).

An incubation period usually precedes the rapid change of properties. It determines the useful service life of the steel and is therefore of particular importance. The incubation period is severely reduced by cold work of the steel prior to exposure to hydrogen and by increased hydrogen pressures (1). The incubation time is increased by certain small alloy additions which segregate to grain boundaries (2), and by carbide stabilizing elements (3): At an advanced stage of attack, when the reactive carbon of the steel becomes exhaused, the rate of attack decreases and the properties approach asymptotically a final value.

The swelling caused by the methane bubbles and fissures may exceed 10 percent of the volume (4). The extent of swelling decreases with increasing concentration of alloy additions such as chromium and molybdenum (2).

The necessity for the presence of carbon to cause attack is indicated by the fact that zone refined iron and decarburized vacuum-melted iron are not attacked. The minimum carbon concentration which still produces observable attack may be very small. The presence of 90 ppm carbon in vacuum-melted iron is sufficient to cause the formation of fissures along grain boundaries (1). Alloy addition to the steel of carbide stabilizers can prevent hydrogen attack even though sufficient carbon is left in solution to cause a limited reaction with hydrogen.

Plastic strain prior to exposure to hydrogen increases the rate of hydrogen attack (1). The action of a steady tensile stress may accelerate hydrogen attack. Kolgatin, et al (5), Chernykh, et al (6), and I. Class (7) performed stress rupture tests using tubular specimens under internal pressure and found a marked reduction of the rupture time by hydrogen for steels ranging from low carbon iron to titanium stabilized austenitic stainless steels. Information on the effect of hydrogen environment on the creep and rupture behavior of solid test specimens is limited. McCoy (8), investigated the creep properties of a large number of different materials including a series of steels in hydrogen environment at atmospheric pressure. His data indicate that atmospheric pressure of hydrogen is insufficient to cause attack. Hofmann and Vogt (9) compared the creep behavior of a low alloy steel in air with that in hydrogen at 100 atm. pressure in the temperature range from 20° to 100°C. This test temperature is in the range of reversible or low strain rate embrittlement rather than that of hydrogen attack. According to Podgurski (10) hydrogen attack by methane formation becomes important above 220°C.

Scope of Investigation and Experimental Program

The purpose of this investigation was to study the effects of hydrogen environment at increased gas pressures on the creep and rupture behavior of steels. The experimental program was designed to obtain information about the mechanism of superposition of hydrogen attack and creep damage as a function of carbon concentration, alloy content, and hydrogen gas pressure.

Creep and stress-rupture tests were performed in argon and in hydrogen atmospheres at 427, 540, and 594°C, selectively for different steels. The majority of the tests was performed at 63 atm. hydrogen pressure; others were conducted at pressures of 28, 85, and 100 atm. The creep properties in hydrogen were compared with those in argon at 3 atm. pressure. Several creep tests were also performed in argon at 100 atm.

Experimental Facilities and Procedures

The creep tests at increased gas pressure were performed in cylindrical, horizontal autoclaves. Figure 1 shows a schematic diagram of one creep testing device in place in an autoclave. The creep testing machine is of the conventicnal lever type, and built

to fit into the autoclave. The specimen is fastened by pins which fit into the holes of the specimen heads. The pins rest on boron nitride sleeves of the loading device. The load is applied to the specimens directly by the lever and the set of weights. The lever rests on an adjustable pivot formed by a steel pin which is seated in two segments of boron nitride sleeves. By changing the number and position of the weights, the initial tensile stress in the specimen can be varied. The base of the loading device is formed by three steel discs which are held together by two rods which penetrate the discs and are fastened by welding. The discs also serve as baffles to minimize the heat loss by convection.

The autoclaves are made from stainless steel type 347 tubes to which large reducers are welded at the ends in order to accommodate the weights and provide sufficient space to permit elongation of the test specimen. Two testing machines are inserted back to back into the autoclave. This positions the test section of the specimens near the center of the autoclave where the temperature is uniform. The autoclave is heated by a cylindrical resistance furnace which has three independent heating elements. The temperature gradient is minimized by adjustment of variable transformers connected with each heating element. The specimen temperature is measured with an inconel-clad thermocouple which extends radially throughout the flange of the autoclave to the specimen.

The creep extension of the specimen is measured from the deflection of the load arm and is indicated by a linear variable differential transformer. The indicating transformer is outside the autoclave; it fits over an austenitic stainless steel tube which is connected to the flange of the autoclave. The iron core of the transformer is connected to the load arm and moves in the steel tube when the load arm is deflecting downwards. The transformer is fixed to a micrometer which permits calibration of the recording system at testing temperature and pressure.

During the preparatory stages of the creep tests the load arm is held by a wire. The load can be applied at test temperature by fusing the wire with an electric current.

Both gases, argon and hydrogen, were prepurified. The hydrogen gas had a dew point of -75°C and contained less than 20 ppm oxygen.

Prior to heating, the autoclaves were evacuated to approximately 0.02 Torr and then purged three times with the gas of the test environment. This procedure was repeated at 150°C to remove adsorbed water from the surfaces of the system.

Test Material

The test materials used range from vacuum-melted decarburized iron (Ferrovac E) to an austenitic 18-8 type stainless steel. The chemical composition and the heat treating temperature of the steels are listed in TABLE I. Ferrovac E iron contained 90 ppm carbon, 80 ppm oxygen, 3 ppm nitrogen, and 0.6 ppm hydrogen. One batch of this material was decarburized to less than 12 ppm carbon. The steels were all commercial grades. The heat treating of the pre-machined test specimens was performed in a vacuum furnace followed by slow cooling.

The test specimens of the steels 5, 3 and 4 had a cross-section of 1.6 x 1.6 mm^2 and those of the materials 1,2,6 and 7, a cross-section of 2.5 x 2.5 mm^2. To obtain a reproducible surface activity in hydrogen, all specimens were polished parallel with the longitudinal axis with 400-grit emery paper just prior to charging.

Experimental Results

Samples of the 18-8 type steel which were exposed in unstressed condition to hydrogen at 63 atm. and 593°C for up to 2100 hours exhibited a 50 percent decrease of the reduction of area and the elongation. However, this embrittlement is reversible since heating in vacuum restored the ductility.

Samples of the materials 1 to 4 were exposed to hydrogen at 63 atm. pressure and 540°C in unstressed condition. Following the exposure, the samples were heated in vacuum at 350°C in order to eliminate the effects of reversible embrittlement. The degree of hydrogen attack was determined from tensile tests of unnotched specimens, bend tests of notched specimens and from the speceific volume increase caused by the expansion of fissures (1). Using equivalent criteria for attack, Ferrovac E iron was attacked in 20 hours, SAE 1020 steel in 60 hours, 0.5% Mo-steel in 1100 hours and the 1% Cr-0.5% Mo-steel in 1800 hours. Although the carbon content of the Ferrovac E was low, small fissures at the grain boundaries were observed microscopically. While the tensile strength properties

of Ferrovac E were not adversely affected by these fissures, they lead to intercrystalline cracks in the notched bend tests, Fig. 2. The decarburized Ferrovac E iron was not affected by exposure to hydrogen.

Stress-rupture curves for the various steels in argon and in hydrogen environments are shown in Figures 3, 4 and 5. Selected values of the reduction of area at fracture are indicated in parentheses. The data for tests in argon show the commonly observed characteristics. For the fracture times investigated, the stress rupture data for the steels No. 5, 3 and 4 can be represented by two straight line segments. The change of the slope indicates a change of the fracture mechanism from transcrystalline to predominantly intercrystalline. This trend is also indicated by the decrease of the reduction of area with increasing rupture time.

For the carbon steel and the two low alloy steels, Figures 3 and 4, all tests carried out in hydrogen resulted in a lower strength than those in argon, over the entire range of fracture times investigated, even for the shortest fracture times measured. Several tests were carried out at different gas pressures. An increase of the pressure of argon from 3 atm. to 100 atm. had no noticeable effect on the rupture time and the creep behavior of the Cr-Mo-steel. The rupture time in hydrogen, however, is progressively reduced as the hydrogen pressure is increased, Fig. 4.

The stress-rupture properties of the 12% Cr-steel were not affected by hydrogen at 63 atm., Fig. 5. The rupture times of the 18-8 type steel were slightly increased by hydrogen, resulting in a parallel displacement of the rupture curve for the stress range which was investigated, Fig. 5.

For the purpose of comparing the effects of hydrogen on the rupture properties of the steels, the ratio of rupture time in argon and that in hydrogen is listed in TABLE II. The ratios are for stresses which resulted in a rupture time of 400 hours in argon. Included in TABLE II is a value for a 2.25% Cr-1% Mo-steel in quenched and tempered condition which is based on a limited number of data.(2)

The effect of hydrogen on the rupture properties of Ferrovac E is low as compared with that on the 0.2% carbon steel, essentially because of the low carbon content of this material. For all the steels

(2) These data obtained through courtesy of Climax Molybdenum Research.

investigated, the effect of hydrogen decreases with increasing alloy content of the steels. The 12% chromium steel is unaffected and the austenitic stainless steel is slightly strengthened by hydrogen.

The minimum creep rate of the steels which are attacked is increased by hydrogen. Examples of creep curves for the low carbon iron are shown in Fig. 6. Ratios of minimum creep rate in hydrogen and in argon at the indicated stress are listed in TABLE II. These ratios increase with increasing rupture time. The ratio of creep rates for the Cr-Mo-steel is comparatively high. This is explained by a selective decarburization in hydrogen atmosphere which resulted in ferrite grain growth and an increase of the ductility of this steel in hydrogen (see Fig. 4).

Examination of the microstructure of carbon steel samples which were exposed to hydrogen in unstressed condition revealed that the nucleation of voids or fissures occurred preferentially at manganese sulfide inclusions. The inclusions remained unattacked. The growth of the fissures occurred in a ductile manner to a spherical shape by a creep mechanism, Fig. 7. The observed embirttlement of the steel is essentially caused by the concentration of strain in the bridges between the fissures, resulting in a low reduction of area of the macroscopic cross section. Decarburization occurred rapidly in the vicinity of the fissures as soon as they assumed a microscopically visible size.

Fissures which formed in the carbon steel during creep in a hydrogen atmosphere were located at grain boundaries rather than at inclusions which extended parallel with the rolling direction. Their orientation was preferred transverse to the applied normal stress, i.e., also transverse to the rolling direction, Fig. 8. The fissures extended only over a few segments of grain boundaries and did not propagate in a brittle manner. The beginning of decomposition of pearlite in the vicinity of fissures and decarburization was observed for specimens which failed in a short time, long before extensive hydrogen attack occurred.

The size and the number of voids which were observed in specimens of the same steel creep tested in argon appeared much later during the creep life at an equivalent stress and were very much smaller than in those tested in hydrogen. The grain boundary voids were observed preferentially at intersections of sub-boundaries and grain boundaries.

The microstructural changes observed in the molybdenum-steel and the chromium-molybdenum steel were in many ways similar to those observed in the carbon steel. The fissures which formed in specimens which were exposed to hydrogen in unstressed condition were smaller in size and more numerous than in the carbon steel. The creep fracture in argon environment was predominantly intercrystalline. For tests in hydrogen, large spherical voids were observed to form in pearlite colonies and near carbides at the grain boundaries. These voids joined by transgranular fracture, Fig. 9.

The creep specimens of the three steels discussed above showed formation of sub-boundaries which became more pronounced with increasing rupture time. A growth of the ferrite grains in hydrogen environment is also evident. This growth of ferrite grains occurred in the Cr-Mo steel in spite of the fact that the microscopically visible carbides were retained. The ferrite grains of the specimens tested in argon remained essentially unchanged.

The microstructure of the 12% chromium-steel showed typical carbide precipitates which remained unchanged by exposure to hydrogen.

Exposure to hydrogen had little effect on the microstructure of the austenitic stainless steel. Carbide extraction replicas indicated continued carbide precipitation during creep testing in hydrogen, particularly along the slip planes near the grain boundaries.

Discussion and Analysis

The effects of hydrogen environment on carbon steels and low alloy steels are essentially caused by the nucleation of methane gas bubbles and their growth to fissures. In unstressed steel the nucleation of the bubbles occurs at interfaces of high energy in the vicinity of carbon sources. These interfaces may be at inclusions or they may be grain boundaries. Segregation of elements which lower the interfacial energy delays the nucleation of bubbles and, thus delays hydrogen attack (2). Plastic deformation during exposure to hydrogen may not only aid the transport of hydrogen to the reaction site but also act by increasing the strain energy at the grain boundaries, thus accelerating hydrogen attack.

The effects of hydrogen on the creep and rupture behavior of steels need to be viewed in terms of the mechanisms which occur in neutral environment. At high stresses, an incremental change of the

stress has a strong influence on the rupture time, and the slope of the curve is small. In this range, the primary mode of deformation is slip; the fracture is ductile and transcrystalline. At lower stresses, a change in the mode of fracture occurs. In this range, grain boundary sliding becomes significant, leading to the formation of grain boundary voids and intercrystalline cracking. The stress sensitivity of the rupture time is lower than that in the high-stress range, resulting in a larger slope of the curve. The stress range at which the slope of the rupture curve changes indicates the test condition at which intercrystalline crack formation becomes noticeable. As the stress is reduced, resulting in increased rupture times, the extent of intercrystalline cracking increases.

The rupture curves for the carbon steel and the low alloy steels in hydrogen environment exhibit the same regions as those observed in argon. However, metallographic examination indicated formation of fissures also in the high stress region. These fissures are similar to those caused by hydrogen attack in unstressed specimens except that the time to produce these is shorter by a factor of several hundred. Plastic deformation in the presence of high-pressure hydrogen essentially accelerates attack.

In the lower stress region, both the stress and the hydrogen attack contribute to formation and growth of fissures, and the behavior can be explained by a superposition of both effects. Hydrogen environment promotes the nucleation of fissures at the grain boundaries, and the methane pressure in the fissures aids the applied stress in the growth of the voids, thus causing a reduction of the rupture time and an increase of the creep rate. The decarburization resulting from hydrogen attack causes a further reduction of the creep strength of the steel.

Summary and Conclusions

The conclusions presented here are only valid for the experimental conditions which were used in this investigation.

Hydrogen environment at increased pressures may affect the creep properties as a solute or by a chemical reaction with the carbon of the steel to form methane. A deterioration of the creep properties occurs when methane is formed at internal reaction sites, leading to high gas pressures in fissures (hydrogen attack). The superimposed effects of the gas pressure in the fissures and of the applied

creep stress causes an increased creep rate and a reduced rupture time. The decarburization resulting from hydrogen attack further lowers the creep properties. Steels which fail in neutral environment by intercrystalline crack propagation may exhibit a ductile, predominantly transcrystalline fracture in high pressure hydrogen environment.

In order that hydrogen attack occurs, the steel must contain in addition to carbon, suitable sites for the methane reaction which permit the nucleation and expansion of fissures. Hydrogen attack is accelerated by creep stress. Steels which are normally not attacked may show signs of hydrogen attack when subjected to a steady stress in hydrogen environment. Increasing alloy concentration of, for example, molybdenum and chromium reduces the effects of hydrogen on the creep properties; the 12 percent chromium steel being completely immune to hydrogen for the test conditions used.

Provided that other conditions are favorable, small concentrations of carbon are sufficient to cause hydrogen attack by methane formation.

The creep properties of an austenitic stainless steel were influenced by hydrogen in solid solution rather than by a chemical reaction. Hydrogen caused increased rupture times, and an embrittlement at room temperature. This behavior may be explained by a lowering of the stacking fault energy by hydrogen.

Acknowledgements

The sponsorship of this work by the Division of Refining of the American Petroleum Institute is gratefully acknowledged. The author thanks Messrs. J. Crawford, E. Holmes and P. Thoma for performing the creep experiments.

References

1. R. E. Allen, R. J. Jansen, P. C. Rosenthal, and F. H. Vitovec, Proc. Am. Petroleum Institute 41, 74 (1961).

2. P. C. Rosenthal, W. L. Schroeder, and F. H. Vitovec, Proc. Am. Petroleum Inst. 43, 98 (1963).

3. F. K. Naumann, Stahl und Eisen, 58, 1239 (1938).

4. F. H. Vitovec, Proc. Am. Petroleum Inst. 44, 179 (1964).

5. N. N. Kolgatin, L. H. Glikman, V. P. Teodorovich, and V. I. Deryabina, Metallovendenie i Termich. Obrabotka Metallov, 3, 19 (1959).

6. N. P. Chernykh, V. D. Molchanova, and M. I. Mil, Issledovaniya Po Zharoprochnym Spiavamn Moscow, 5, 98 (1959).

7. I. Class, Stahl und Eisen, 80, 1117 (1960).

8. H. E. McCoy, Jr., USAEC, ORNL-3600, June 1964.

9. W. Hofmann and J. Vogt, Arch. f. d. Eisenhüttenwesen, 35, 551 (1964).

10. H. H. Podgurski, Trans. AIME, 221, 389 (1961).

TABLE I

Chemical Composition and Heat Treating

Temperature of Test Materials

No.	Test Material	Concentration of Elements w/o								Heat Treating Temp. °C
		C	Mn	Si	S	P	Mo	Cr	Ni	
1	Ferrovac E, Dec.	0.001	0.001	0.006	0.007	0.002	0.01	0.01	0.04	927
2	Ferrovac E	0.009	0.001	0.006	0.007	0.002	0.01	0.01	0.04	927
3	SAE 1020	0.21	0.52	0.04	0.032	0.015	n.d.	0.04	0.04	900
4	0.5 Mo	0.13	0.41	0.21	0.025	0.017	0.45	0.07	n.d.	955
5	1 Cr - 0.5 Mo	0.10	0.46	0.80	0.010	0.011	0.53	1.14	n.d.	927
6	12 Cr, Type 410	0.15	0.39	0.51	0.005	0.030	0.03	12.28	0.48	855
7	18-8, Type 302	0.090	1.56	0.38	0.015	0.020	0.03	17.86	8.86	1100

TABLE II

Effect of Hydrogen on the Rupture Time

of Various Steels

Test Material	Carbon Content w/o	Test Temp. °C	Ratio of Rupt. Times +) Ar/H_2	Stress +) kg/mm²	Ratio $\dot{\varepsilon}_H/\dot{\varepsilon}_{Ar}$
Ferrovac E, Dec.	0.001	540	1	2.7	1
Ferrovac E	0.009	540	4	3.0	2
SAE 1020	0.21	540	27	11.0	-
0.5% Mo	0.13	540	12.2	26.7	18
1% Cr - 0.5% Mo	0.10	540	11.5	30.2	30
2.25% Cr - 1% Mo	0.13	540	2	38.3	14
12% Cr	0.15	594	1	8.1	1
18% Cr - 8% Ni	0.09	594	0.7	25.5	0.7

+) Stress for Rupture Time of 400 hr. in Argon.
Argon Pressure 3 atm., Hydrogen Pressure 63 atm.

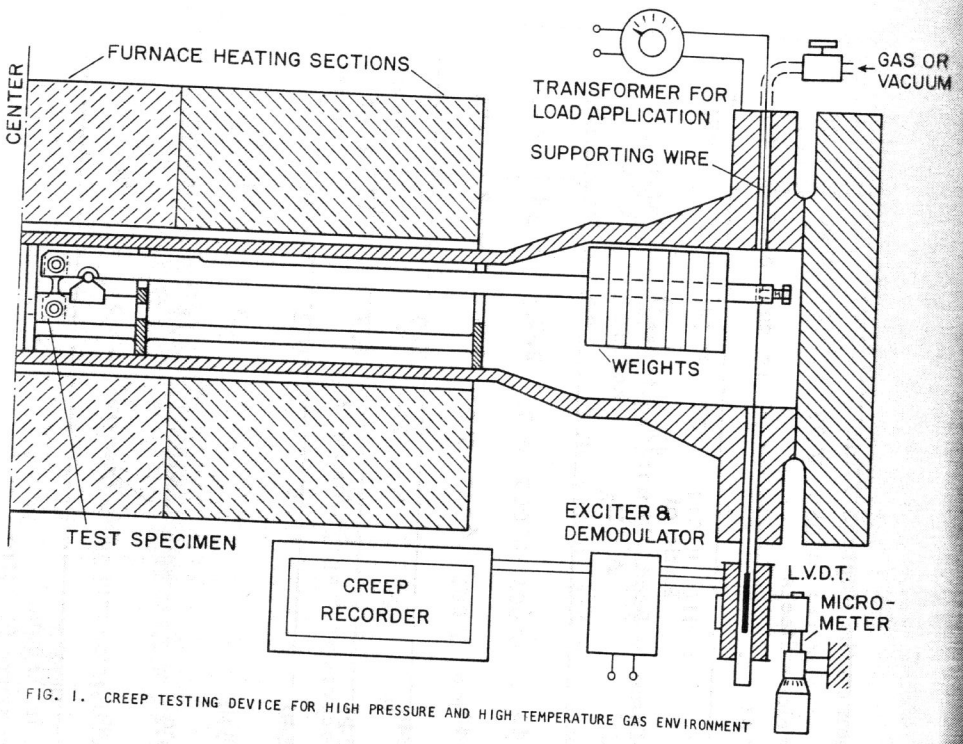

FIG. 1. CREEP TESTING DEVICE FOR HIGH PRESSURE AND HIGH TEMPERATURE GAS ENVIRONMENT

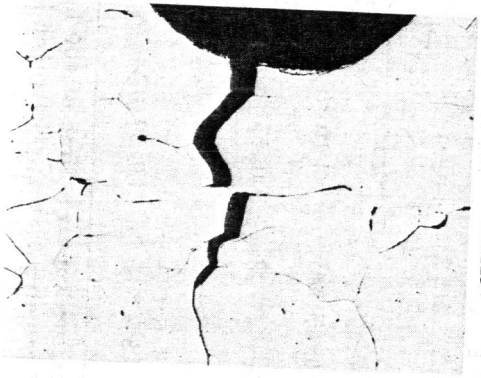

FIG. 2.

INTERCRYSTALLINE CRACK PROPAGATION IN A NOTCHED BEND SPECIMEN OF A LOW-CARBON IRON (FERROVAC E) AFTER 245 HOURS OF EXPOSURE TO HYDROGEN AT 63 ATM PRESSURE AND 540° C TEST TEMPERATURE. 74X

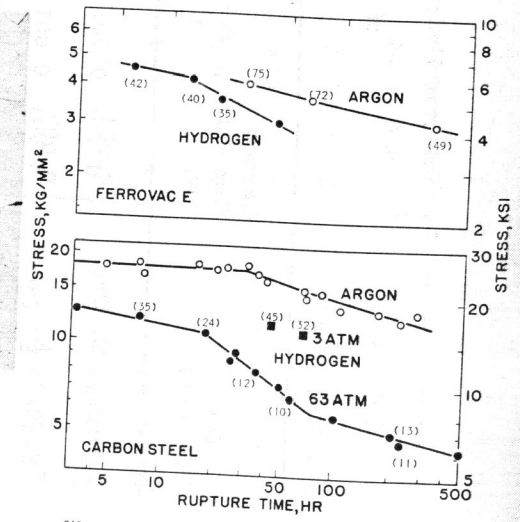

FIG. 3. STRESS-RUPTURE CURVES FOR THE LOW-CARBON IRON AND THE CARBON-STEEL IN ARGON AT 3 ATM AND HYDROGEN AT 63 ATM AT 540° C.

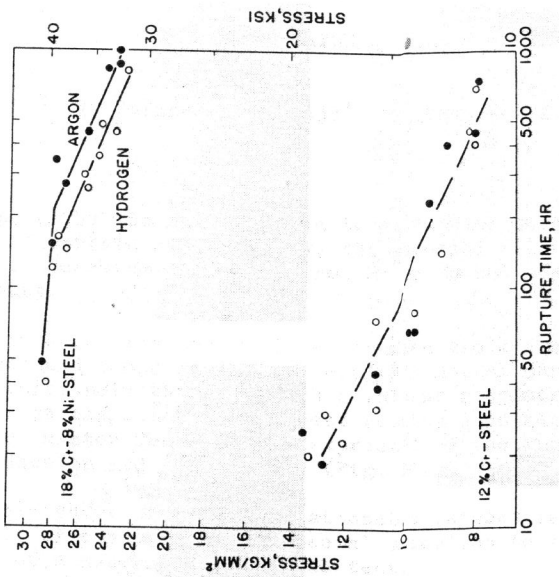

FIG. 5. STRESS-RUPTURE CURVES FOR THE CHROMIUM-STEEL AND THE CHROMIUM-NICKEL STEEL IN ARGON AT 3 ATM AND HYDROGEN AT 63 ATM AT 594° C.

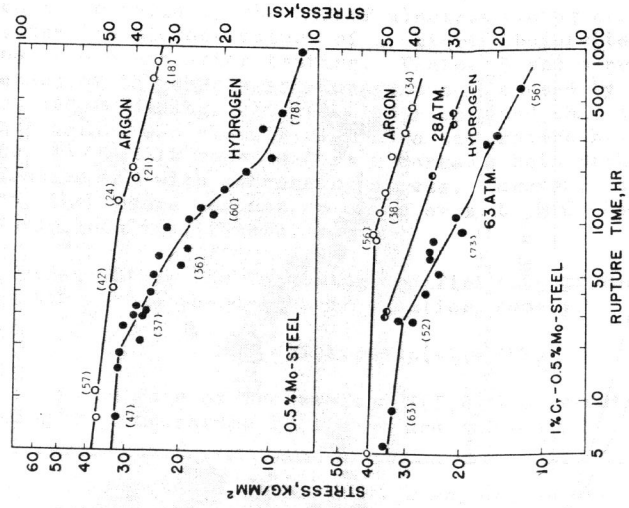

FIG. 4. STRESS RUPTURE CURVES FOR THE MOLYBDENUM-STEEL AND THE CHROMIUM-MOLYBDENUM STEEL IN ARGON AT 3 ATM AND HYDROGEN AT 63 ATM AT 540° C.

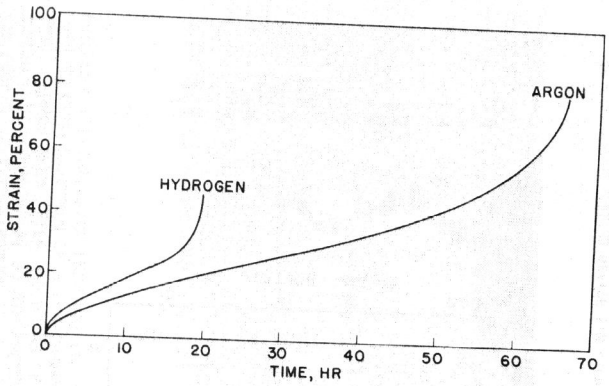

FIG. 6. EXAMPLE OF CREEP CURVES FOR THE LOW-CARBON IRON (FERROVAC E) IN ARGON AT 3 ATM AND HYDROGEN AT 63 ATM PRESSURE, 3.6 KG/MM^2 STRESS AND 540° C TEST TEMPERATURE.

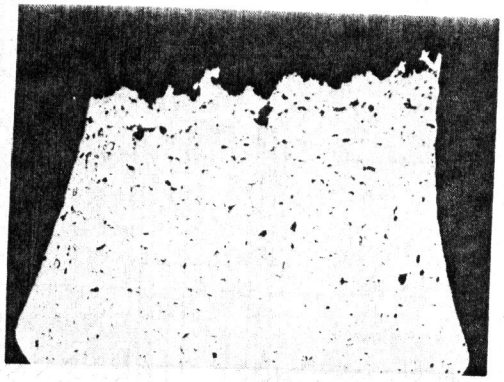

FIG. 8. FISSURE DISTRIBUTION AND FRACTURE IN A CARBON-STEEL CREEP SPECIMEN TESTED IN HYDROGEN AT 100 ATM PRESSURE. 38X

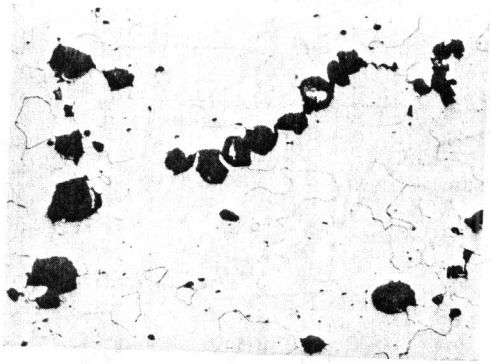

FIG. 7. TYPICAL FISSURES WHICH RESULTED FROM JOINING OF GAS BUBBLES IN ANNEALED CARBON-STEEL CAUSED BY 245 HOURS OF EXPOSURE TO 63 ATM HYDROGEN AT 540° C. 76X

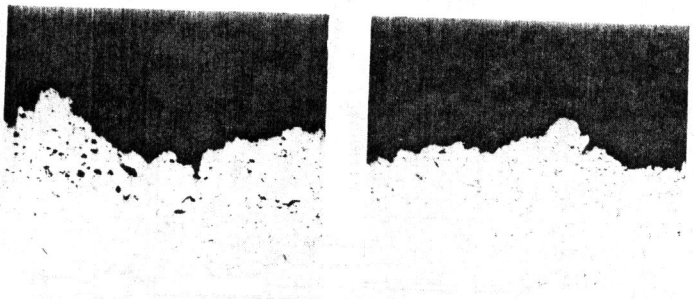

14.5 HOURS RUPTURE-TIME IN HYDROGEN 146 HOURS RUPTURE-TIME IN ARGON

FIG. 9. DISTRIBUTION OF FISSURES IN THE VICINITY OF THE FRACTURE IN THE CHROMIUM-MOLYBDENUM STEEL. BOTH TESTS WERE AT A STRESS OF 38 KG/MM2 AND AT 540° C. (LIGHTLY ETCHED.48X)